

# A Robust Inverse Method Based on Least Square Support Vector Regression for Johnson-cook Material Parameters

Hu Wang<sup>1</sup>, Weiyi Li<sup>1</sup> and Guangyao Li<sup>1</sup>

**Abstract:** The purpose of this study is to propose a robust inverse method for estimating Johnson–Cook material parameters. The method is shown through illustrative examples for two different advanced high strength steel (AHSS) materials (DP980 and TRIP780) using set of data from impact experiments with different velocities. Compared with widely mixed numerical experimental methods, the suggested inverse method has the capability to guarantee the robustness of the obtained parameters by considering uncertainties. The inverse problem is converted into multi-objective optimization problems. Furthermore, in order to improve the performance in efficiency and accuracy, metamodeling techniques and global optimization method are integrated. The final results demonstrate that the experimental and simulation curves are well matched based on identified by the suggested robust inverse method.

**Keywords:** Robust inverse method, John-Cook model, metamodel, least square support vector regression

## 1 Introduction

The lightweight of auto bodies is becoming the popular tendency in the automobile design to respond the world-wide consciousness of environmental protection. The advanced high strength steels (AHSS), which have good performance and low cost compared to the other light weighting materials, have been extensively used in the auto bodies. The experimental results for AHSS at high strain rates show that the yields and plastic hardened process are obviously different from those at low strain rates [Mangono(1999)]. Therefore, identification the accurate material parameters might pose a challenge. The most common method to evaluate the material parameters is by standard tensile tests. However, the simple experiments don't consider the complex loading conditions and the strain rate is not uniform during loading

---

<sup>1</sup> State Key Laboratory of Advanced Design and Manufacturing for Vehicle Body, Hunan University, Changsha, 410082, China

procedure [Langrand et al(1999)]. In order to identify the material parameters of the AHSS model accurately, an inverse method by combining experiments with FE simulations as the mixed numerical experimental methods (MNEM) [Ghouati and Gelin (1997, 2001); Kajberg and Lindkvist(2004)] has now become possible to characterize the deformation behavior under complex loading conditions with much higher accuracy than ever. These inverse methods offer a powerful tool to identify all kinds of unknown parameters in a numerical model, e.g. a FE model. In the past several attempts have been made to identify material parameters based on inverse modeling of different experimental set-ups. Some scholars have used a transversely loaded rectangular plate, a circular disk under diametrical compression and the displacement information around a hole in a biaxial loaded plate to identify the material parameters [Molomard et al.(2005); Wang and Kam(2004); Wang et al.(2005); Cardenas-Garcia et al.(2005)]. Furthermore, others use the boundary element method (BEM) [Huang et al. (2004)] or the virtual field method (VFM) [Grediac (2005)] instead of the finite element method (FEM), but the overall principle remains identical.

Although different implementations of inverse methods have corresponding advantages and characterizes, in most of them the (material) parameters can be iteratively determined by minimizing a cost function which expresses the difference between the experimental and computed response of the physical system under study, e.g. by comparing displacement fields, strain fields, resonant frequencies, etc.[Langrand et al (1999); Dey et al.(2007)]. These inverse methods commonly don't consider the uncertain factors, such as experimental environment, accuracy of simulation procedure, especially for high strain rate cases. Thus, the MNEMs can successfully obtain the material parameters by considering the complex loading, the robustness of the material parameters cannot be guaranteed. According to the reports from different research organizations, the material parameters related dynamical test are far from homogenous, even if the test specimen are from the same batch. It is necessary to establish a robust inverse method for high strain related material identification.

In this study, we focus the identification of parameters of Johnson–Cook (JC) material model [Johnson and Cook (1983)]. This material model is one of the most widely used models because it takes on a simple, yet effective. The key issue of this study is to develop a robust inverse method. In order to consider uncertainties during identification, the inverse method is moved from a single objective optimization to a multi-objective optimization. Furthermore, for the sake of accuracy and efficiency, some strategies, such as global optimization and metamodeling techniques, are also employed. The rests of this paper is organized as follows. The JC model is introduced in Section 2. In section 3, a robust inverse method is presented. Some important issues, least square support vector regression (LS-SVR), intelligent sam-

pling strategy and multi-objective optimization are also suggested in Section 3.1, 3.2, 3.3 and 3.4, respectively. In section 4, the proposed inverse method is applied for the material parameters of AHSS.

## 2 Johnson-Cook model

The JC material model is one amongst many other semi-empirical constitutive models which describe the plastic material behavior at high strains, at high strain rates and at high temperatures. Using the JC model, the flow stress can be expressed as:

$$\sigma = (A + B\varepsilon_{pl}^n) \left( 1 + C \ln \frac{\dot{\varepsilon}_p}{\dot{\varepsilon}_0} \right) [1 - (T^*)^m] \quad (1)$$

where  $\sigma$  is the equivalent stress response;  $\varepsilon_p$  and  $\dot{\varepsilon}_p$  are the equivalent plastic strain and strain rate, respectively;  $\dot{\varepsilon}_0$  is a normalizing reference strain rate;  $A$  and  $B$  are the strain hardening parameters, where  $C$  is a dimensionless strain rate hardening coefficient. Parameters  $n$  and  $m$  are power exponents of the strain hardening and thermal softening terms;  $T^*$  is a normalized temperature as

$$T^* = \frac{T - T_{room}}{T_{melt} - T_{room}} \quad (2)$$

where  $T$  is the current temperature of the material,  $T_{melt}$  is the melting point of the material and  $T_{room}$  is the room temperature.

## 3 Robust inverse method

It is well known, the performance of MNEM is heavily relies on the efficiency, accuracy and stability of FE simulation. There are three challenges for construction of a robust inverse method, global optimum, efficiency and reliability.

For searching the global optimum results, the heuristic search method based on the evolution algorithms (EA), such as genetic algorithms (GAs) was introduced to overcome local convergence several decades ago [Holland(1975), Goldberg(1989)]. Despite the fact that the use of EA is not novel with regard to the cited literature, it is still considered as an attractive way in solving several problems related to engineering design and material parameter identification. However, the well-known weakness is that they require a high number of evaluations and are difficult to use for real engineering problems. A way for keep cost as low as possible is through the use of surrogate evaluation tool, so called metamodel. Therefore, the metamodel-based optimization which can be applied for global optimization with limited time-consuming evaluation is introduced for inverse method. Compared with traditional EA strategy, the computational cost should be reduced significantly. However, the

metamodel would decrease the accuracy of optimization. Furthermore, the robustness of the metamodel should be considered simultaneously. Since the metamodel-based optimization is used for inverse method, the accuracy and robustness of the FE simulation and metamodel should be addressed.

Due to the defects of the numerical algorithm and uncertain factors of the simulation, noisy and outlier points might approach during inversion procedure. Thus, interpolation-based metamodeling techniques, such as Kriging and RBF which pass through all sample points, cannot screen out the noise and outliers. Although the RS-based metamodel can construct smooth models, the drawback of using second-order RS models is that they may not be appropriate for building global models over the entire design space for highly nonlinear problems. They might not be effective or appropriate for material parameter identification. Therefore, the metamodel-based inverse method requires behaving the capability for filter the interference of noise.

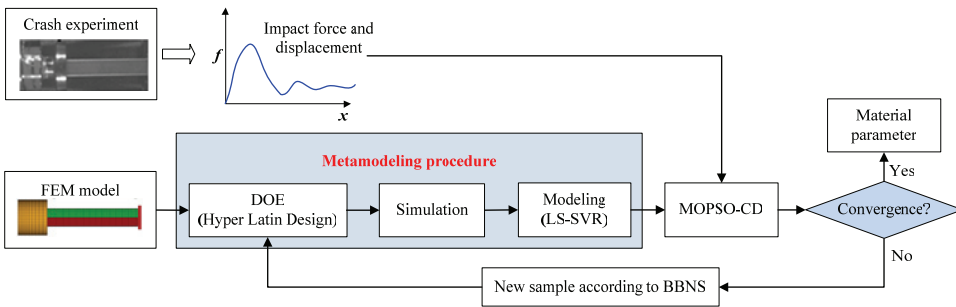


Figure 1: The basic flowchart of the robust inverse method

In summary, the robust metamodel-based inverse method should have following properties as: high efficiency, accuracy and robustness. Based on these requirements, the flowchart of the robust inverse method is suggested as Fig.1. The basic frame of the suggested method is described as:

1. The Latin hypercube design (LHD) is used for generating the initial samples for construction of metamodel;
2. The initial samples are substituted into FE model and evaluated by FE simulations;
3. The LS-SVR is used for construction of the robust model based on generated samples;

4. The multi-objective particle swarm optimization with the robust model is used for determining the material parameters;
5. The obtained material parameters should be substituted into the FE model to obtain the corresponding response;
6. Checking the convergence condition;
7. If procedure converges, the new sample should be generated by the boundary-based neighbor sampling strategy and procedure goes to Step 3.

According to the robust method, several techniques are used for improving the accuracy, efficiency and robustness of the proposed method. The details and reasons are presented as following sections.

### 3.1 Least square support vector regression (LS-SVR)

In order to achieve the robust and accurate model, least square support vector regression (LS-SVR) is employed to construct model. Compared with empirical risk minimization (ERM)-based approximation techniques (such as Kriging, LS, moving least square methods), the LS-SVR is based on the structure risk minimization (SRM) and derived from support vector regression (SVR). Unlike traditional methods which minimize the empirical training error, the SVR aims to minimize the upper bound of the generalization error through maximizing the margin between the separating hyperplane and data. Recently, several studies [Yang H et al. (2002a, 2002b); Wu et al. (2003); Cherkassky and Ma (2004)] have successfully applied the SVR to the function estimation. Recently, a least squares version of the SVR called as least square SVR (LS-SVR) technique has received some attention for curve estimation. In the LS-SVR, Vapnik's  $\varepsilon$ -insensitive loss function has been replaced by a sum-squared error (SSE) cost function. Moreover, the LS-SVR considers equality type constraints instead of inequalities as in the traditional SVR approach. This reformulation greatly simplifies a problem such that the LS-SVR solution follows directly from solving a set of linear equations rather than from a convex quadratic program (QP) [Suykens and Vandewalle (1999)]. For these reasons, the LS-SVR approximation can achieve more robust and objective stress-strain curve theoretically [Wang et al. (2010)]. The details of the LS-SVR are described as follows.

Considering a given training set of  $N$  sample points  $\{x_i, y_i\}_{i=1}^N$  with the input data  $x_i$  and output data  $y_i$  presented as

$$D = \{(x_1, y_1), (x_2, y_2) \cdots (x_i, y_i) \cdots (x_N, y_N)\}, x_i \in R^n, y_i \in R. \quad (3)$$

The optimization problem in primal weight space is expressed as

$$\text{Min}_{w, \varepsilon} J(w, \varepsilon) = \frac{1}{2} w^T w + \frac{1}{2} \gamma \sum_{i=1}^N \varepsilon_i^2 \quad (4)$$

subjected to the constraint

$$y_i = w^T \varphi(x_i) + b + \varepsilon_i, i = 1, 2, \dots, N \quad (5)$$

where  $\varphi(\cdot)$  is a kernel function that maps the input space into a so-called higher dimensional feature space. Here,  $w$  denotes the weight vector in primal space,  $\varepsilon_i$  is error variable and  $b$  is the bias term. The cost function  $J$  consists of a sum squared error (SSE) fitting error and regulation term. The relative importance of the empirical risk minimization and structural risk minimization terms is determined by the positive constant  $\gamma$ .

The model of primal space is presented as follows

$$y(x) = w^T \varphi(x) + b. \quad (6)$$

The weight vector  $w$  can be of infinite dimension, which makes a calculation of  $w$  from Eq.4 impossible in general. Therefore, we can compute the model in the dual space instead of the primal space. Then, the Lagrangian multiplier expression applied to Eqs.(4-6) is obtained as

$$\ell(w, b, \varepsilon, a) = J(w, \varepsilon) - \sum_{i=1}^N a_i \{w^T \varphi(x_i) + b + \varepsilon_i - y_i\} \quad (7)$$

with  $a_i$  being the Lagrangian multipliers. The criteria satisfied by the optimal solution can be given as

$$\begin{cases} \frac{\partial(\ell(w, b, \varepsilon, a))}{\partial w} = 0 \rightarrow w = \sum_{i=1}^N a_i \varphi(x_i) \\ \frac{\partial(\ell(w, b, \varepsilon, a))}{\partial b} = 0 \rightarrow \sum_{i=1}^N a_i = 0 \\ \frac{\partial(\ell(w, b, \varepsilon, a))}{\partial \varepsilon} = 0 \rightarrow a_i = \gamma \varepsilon_i \\ \frac{\partial(\ell(w, b, \varepsilon, a))}{\partial a} = 0 \rightarrow w^T \varphi(x_i) + b + \varepsilon_i - y_i = 0 \end{cases} \quad (8)$$

Eliminating of  $w$  and  $\varepsilon$ , the solution is determined by

$$\begin{bmatrix} 0 & I^T \\ I & \Gamma + \frac{1}{\gamma} I \end{bmatrix} \begin{bmatrix} b \\ a \end{bmatrix} = \begin{bmatrix} 0 \\ y \end{bmatrix}, \quad (9)$$

where

$$y = [y_1; y_2; \dots y_N], \tag{10}$$

$$I = [1; 1; \dots 1], \tag{11}$$

$$a = [a_1; a_2; \dots a_N], \tag{12}$$

$$\Gamma_{i,j} = \varphi(x_i)^T \varphi(x_j) \text{ for } i, j = 1, 2, \dots N. \tag{13}$$

The resulting LS-SVR model for the function estimation is then

$$y(x) = \sum_{i=1}^N a_i K(x, x_i) + b, \tag{14}$$

where  $a_i$  and  $b$  are the solutions of Eq.(9). For  $K(\cdot, \cdot)$ , we typically has the following choices,  $K(x, x_i) = x_i^T x$ (linear),  $K(x, x_i) = (x_i^T x + 1)^m$  (polynomial with degree  $m$ ),  $K(x_i, x) = \exp\left(-\|x_i - x\|^2 / \sigma^2\right)$ (RBF). This study focuses on the selection of RBF kernel map.

When solving large linear systems, it is often necessary to apply iterative methods to Eq.(9). However, the matrix in Eq.(9) is not positive definite. It is required to transform the system into a positive definite matrix, and iterative methods (conjugate gradient, successive over relaxation or others) can be applied to it. However, the conjugate gradient method for solving a linear system has high computational complexity. The speed of convergence depends on the condition number of matrix. In the case of the LS-SVR, the accuracy of approximation is influenced by the choice of  $\gamma$  and  $\sigma$  when using an RBF kernel.

### **3.2 Intelligent sampling strategy**

In order to further control the computational cost, an intelligent sampling strategy is integrated with the LS-SVR. Sampling strategy actually is design of experiment (DOE). The intelligent design of experiments (DOE) is used to control the number of sample points and reduce initial design space. An active branch of research in metamodeling techniques is online sampling strategies that can reduce design space to improve the accuracy of metamodels. Box and Draper (1969) suggested a method to refine the response surface to capture real function by screening out unimportant variables. Chen, et al (1997) suggested heuristics to lead the surface refinement to a smaller design space. Wujek and Renaud(1998a, 1998b) compared several move-limit strategies that focus on controlling function approximation in a more meaningful design space. Toropov and his cooperators (1996) suggested a sequential metamodeling approach. This method is integrated with move limits

and trust regions strategies by Alexandrov (1998). Wang (2001) advanced fuzzy clustering based hierarchical metamodeling for design space reduction and optimization. Wang and Li (2008a, 2008b) developed particle swarm optimization intelligent sampling (PSOIS) and boundary and best neighbor sampling (BBNS) for enhancing the accuracy and efficiency of metamodel respectively. In this work, the BBNS is integrated with the suggested inverse method for material identification. The details of the BBNS are presented as

Commonly, bounds of design variables can be well defined according to rich engineering experience. The characteristic of the BBNS is to use bounds of design variables and better sample points of design space to generate new sample points. Firstly, initial sample points should be generated by popular DOEs, such as full factorial (FF), D-optimum (D-OPT), LHS, etc. To save computational expense of evaluations, the initial sample points should be sparsely distributed. Sequentially, experiments should be performed with the existing sample points and values of corresponding objective functions should be obtained. And then, the sample points are sorted according to the descending order of their objective functions. The several sample points which are on the top of the sorted list are collected as a new initial sample set. The new initial sample point is used to position the new sample point based on the nearest boundary sample point and the best neighbor sample point till convergence. The BBNS searching pattern is illustrated in Fig.2.

The details of the BBNS are described as follows:

Step 1. Choose a popular DOE (such as LHS) to generate a sparsely distributed initial sample set. The boundary sample points are also created.

Step 2. Perform preliminary design evaluations (simulations) with the initial sample points. In this step, the boundary sample points do not require evaluation. The evaluations with the boundary sample points should be performed in Step 4 when the closest boundary sample points are assigned.

Step 3. Sort the sample points in descending order based on objective functions. Collect the top of several sample points on the sorted list. The collected sample point can then be called a “better sample” and a set of better sample points can be called a “better-sample-set” (as Figure.2 shows).

Step 4. Generate the new sample point according to Eq. (15-16)

Step 4.1 The value of the new sample point is then given by

$$X_{1,2,\dots,n} = \left( \frac{X_{1,2,\dots,n}^{Current} + X_{1,2,\dots,n}^{Boundary(Nearest)}}{m1_{1,2,\dots,n}} \right) c_1 + \left( \frac{X_{1,2,\dots,n}^{Current} + X_{1,2,\dots,n}^{Best(Nearest)}}{m2_{1,2,\dots,n}} \right) c_2 \quad (15)$$

where  $X$  is the coordinate vector of sample point,  $n$  denotes the number of design



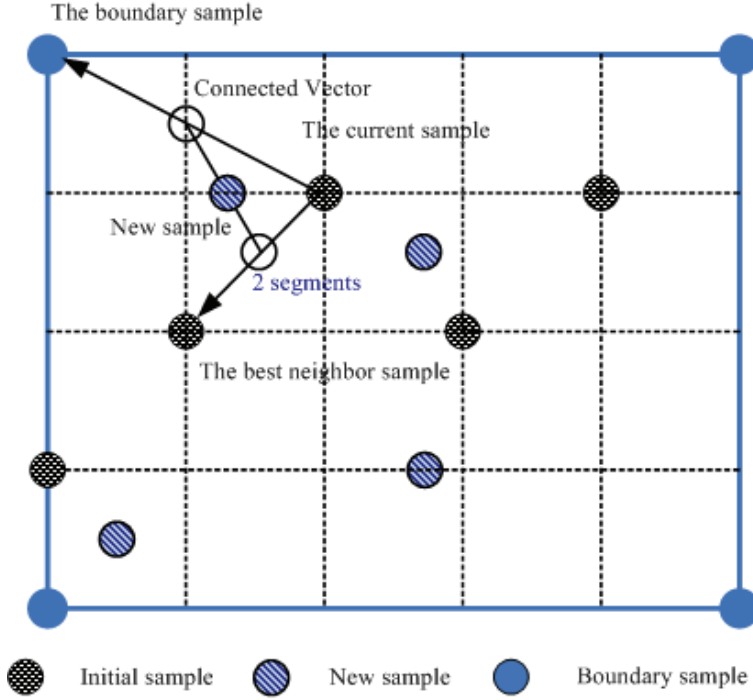


Figure 2: An illustration of BBNS searching pattern [Wang et al.(2008b)]

variables,  $m1$ , and  $m2$  are determined by

$$\begin{cases} m1_{1,2,\dots,n} = \frac{R(x_{1,2,\dots,n}^{Current}) + R(x_{1,2,\dots,n}^{Boundary(Nearest)})}{R(x_i^{Boundary(Nearest)})} \\ m2_{1,2,\dots,n} = \frac{R(x_{1,2,\dots,n}^{Current}) + R(x_{1,2,\dots,n}^{Best(Nearest)})}{R(x_{1,2,\dots,n}^{Best(Nearest)})} \end{cases} \quad (16)$$

$c_1, c_2$  denote acceleration weight coefficient vectors, which are determined by

$$\begin{cases} c_1 = \frac{R(X_{1,2,\dots,n}^{Current}) + R(X_{1,2,\dots,n}^{Boundary(Nearest)})}{(R(X_{1,2,\dots,n}^{Current}) + R(X_{1,2,\dots,n}^{Boundary(Nearest)})) + (R(X_{1,2,\dots,n}^{Current}) + R(X_{1,2,\dots,n}^{Best(Nearest)}))} \\ c_1 = 1 - c_2 \end{cases} \quad (17)$$

where  $R(\cdot)$  denotes the response of the objective function, such as  $v_{1,2,\dots,n}^{Best}$ ,  $v_{1,2,\dots,n}^{Boundary(Nearest)}$  and  $v_{1,2,\dots,n}^{Best(Nearest)}$ .

The meaning of superscripts is as follows:

*Current* the current sample in the better sample set

*Nearest* the nearest sample from the current sample point

*Boundary* boundary of the intervals (constraints)

*Best* the sample which has the best value of objective function

*Boundary (nearest)* boundary sample point closest to the nearest one

*Best (nearest)* sample closest to the best sample set

Step 4.2 If the position of the new sample point is duplicated (occupies an existing one) or is located outside of the design space, substitute the best sample point of last iteration with the current assigned one, and return to Step 4.1 in the procedure;

Step 4.3 Perform the evaluations (simulations) with the new sample points;

Step 4.4 Update the best sample set.

Step.5 If

$$\frac{|R(v_{new}^{Best}) - R(v_{old}^{Best})|}{|R(v_{new}^{Best})|} \leq \eta, \eta \in (0, 1), \tag{18}$$

then procedure ends. If not, proceed to Step 3, where  $\eta$  is the threshold which can be set by the user, with the default value given as 0.1.

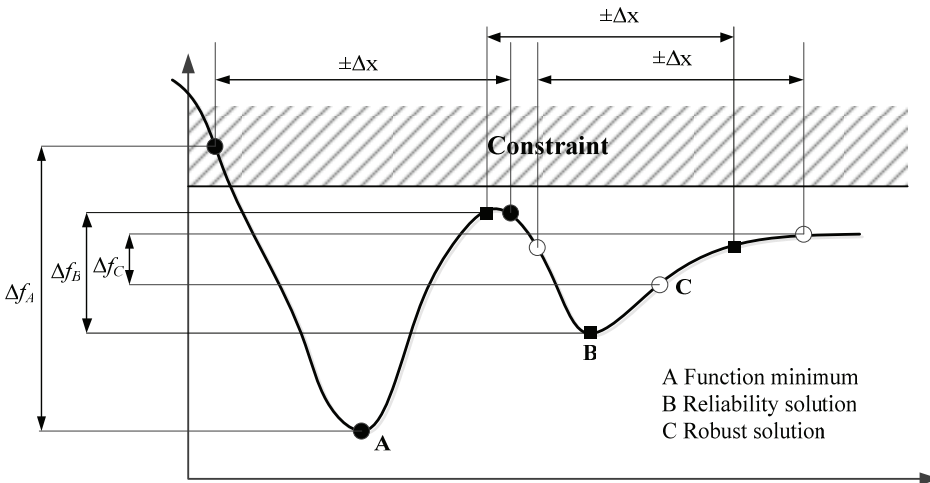


Figure 3: Schematic of robust inverse method

### 3.3 Robust inverse method

For material parameter identification, the objective function of the inverse method is to minimize the gap between the experimental and the numerical results. The popular inverse method does not consider influence due to the uncertainties of the experimental environment. The robust inverse method develops a solution that is insensitive to variations of the nominal design and is feasible in an uncertainty range around the nominal design. As shown in Fig.3, the X-axis represents the uncertainty factors, involving parameters need to obtain and noise factors, and the vertical axis represents the value of objective function  $f(x)$  to be minimized (such as the gap between the experimental and the numerical results). According to Fig.3, solution **C** of the **A**, **B**, and **C** should be considered robust one as a variation of  $\pm\Delta x$  in unknown parameter does not alter the objective function too much and maintains the solution within the design space when the unknown parameters are perturbed. Although Solution **B** is also within the design space when the design variables vary in  $\pm\Delta x$ , the perturbation causes a larger change in objective function. Solution **A** is highly sensitive to the parameter perturbation and often cannot be recommended in practice, even though it has a better mean value than Solutions **A** and **B**. It is noted that there are more robust solutions than solution **C** on the right of solution **C**, but the objective performance must be compromised. Therefore, the robustness and objective performance should be taken into account simultaneously in the mathematical formulation and corresponding general robust inverse problem can be presented as

$$\begin{cases} \min \{f_1(Y_\mu(X), Y_\sigma(X)), f_2(Y_\mu(X), Y_\sigma(X)) \cdots f_n(Y_\mu(X), Y_\sigma(X))\} \\ s.t. \ g_{\mu j}(X) + \eta g_{\sigma j}(X) \leq 0 \\ X^L + \eta X_\sigma \leq X_\mu \leq X^U - \eta X_\sigma \end{cases} \quad (19)$$

where  $n$  is the number of objective functions,  $Y_\mu(X)$  and  $Y_\sigma(X)$  denote the mean values and standard deviations (STD) of objective functions, respectively.  $g_{\mu j}(X)$  and  $g_{\sigma j}(X)$  denote the mean value and STD of the  $j$ th constraint, respectively.  $X^L$  and  $X^U$  are the lower and upper bounds of the vector  $X$ ,  $X_\mu$  and  $X_\sigma$  are mean value and STD OF  $X$ , and  $\eta=6$  denotes the six sigma design.

For the minimization problem aiming to minimize the function mean by expressing the objective function as follow.

$$f_i(Y_\mu(X), Y_\sigma(X)) = wY_\mu^2(X) + (1 - w)Y_\sigma^2(X) \quad (20)$$

where  $w$  denotes the weight to emphasize the mean or STD values.

### 3.4 Multi-objective particle swarm optimization method

The PSO is a stochastic optimization technique recently introduced by Kennedy and Eberhart(1995), which is inspired by social behavior of bird flocking and fish schooling [Kennedy and Eberhart (1995)]. The PSO is a population-based search method, which exploits the concept of social sharing of information.

This means that each individual (called particle) of a given population (called swarm) can profit from the previous experiences of all other individuals from the same population. During the search process in the solution space, each particle (i.e., candidate solution) will adjust its flying velocity and position according to its own flying experience as well as the experiences of the other companion particles of the swarm. PSO has been shown to be promising for solving various engineering problems.

In the PSO, each particle has a position  $X = (x_1, x_2, x_3, \dots, x_D)$  and a velocity  $V = (v_1, v_2, v_3, \dots, v_D)$  in the variable space. In generation  $t+1$ , the updated velocity and position should be as follows:

$$v_{id}^{t+1} = wv_{id}^t + c_1r_1(p_{id}^t - x_{id}^t) + c_2r_2(p_{gd}^t - x_{id}^t) \quad (21)$$

$$x_{id}^{t+1} = x_{id}^t + v_{id}^{t+1} \quad (22)$$

where  $i = 1, 2, \dots, N$  and  $N$  is the population size;  $d = 1, 2, \dots, D$  and  $D$  denotes the dimension of the search space;  $w$  is the inertia weight factor;  $c_1$  and  $c_2$  are two positive constants;  $r_1$  and  $r_2$  are random uniformly distributed in the range  $[0,1]$ ;  $p_{gd}^t$  and  $p_{id}^t$  denote the global and the personal best of the population, respectively. The performance of each particle is measured according to a pre-defined fitness function which relates to the problem concerned. The inertia weight  $w$  is employed to control the impact of the previous velocities on the current one; hence it influences the trade-off between the global and the local exploration abilities of the particles [Shi and Eberhart (1998)]. In this work, the inertia weight  $w$  is set as 0.4[Coello (2004)].

According to Eq.(19), the objective function can be transformed to multi-objective function as

$$\min \{f_1(Y_\mu^2(X), Y_\sigma^2(X)), f_2(Y_\mu^2(X), Y_\sigma^2(X)) \dots f_n(Y_\mu^2(X), Y_\sigma^2(X))\} \quad (23)$$

Therefore, the robust inverse method should be regarded as multi-objective optimization method.

As an extension to the PSO, the multi-objective particle swarm optimization incorporating the mechanism of crowding distance computation (MOPSO-CD)[ Raquel

and Naval (2005)] has drawn some attention recently as it exhibits a relatively fast convergence and well-distributed Pareto front compared with other multi-objective optimization algorithms, the most recent techniques like NSGA-II [Deb et al. (2002)], SPEA-2 [Zitzler et al.(2001)] and PESA-II [Corne et al. (2001)]. Therefore, The MOPSO-CD is used to obtain the robust material parameters in this work. A diagram of the MOPSO-CD is presented in Fig.4. The details of MOPSO-CD can be consulted in Ref. ) [ Raquel and Naval (2005)].

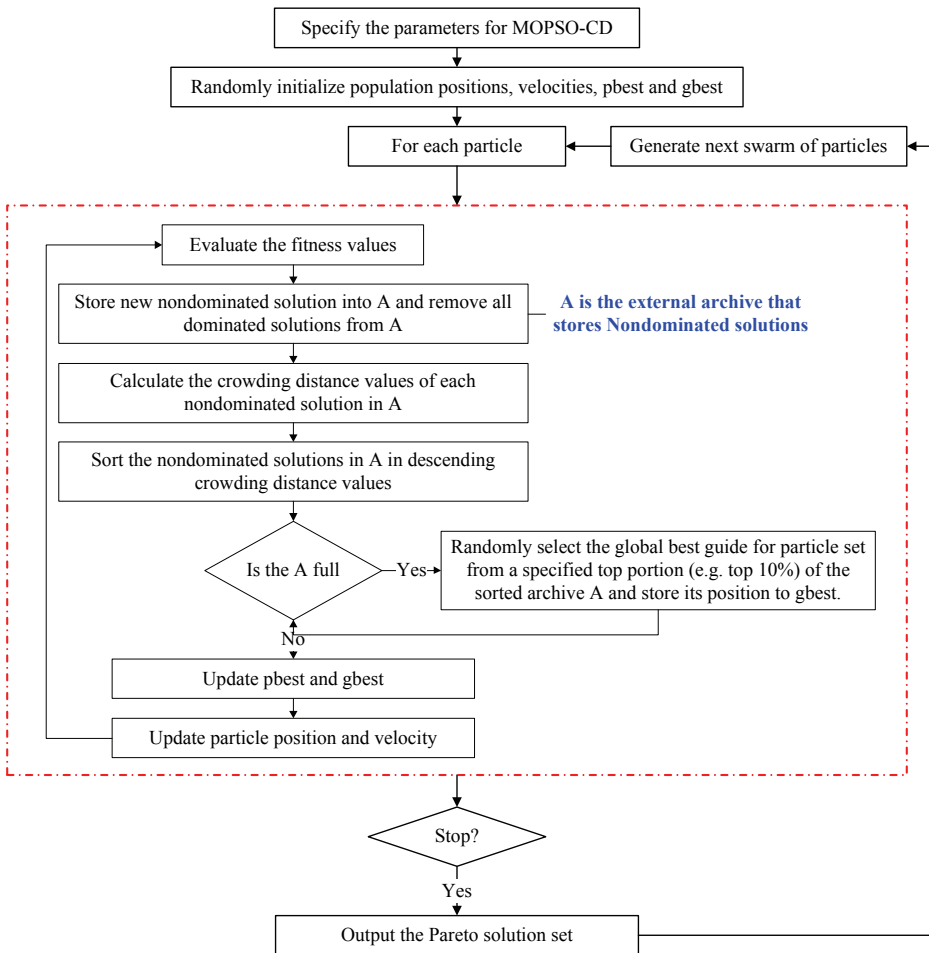


Figure 4: An illustration of MOPSO-CD algorithm

#### 4 Applications for advanced high strength stiffness steels

This work is concerned about two types of AHSS; Dual Phase (DP) steels and Transformation-Induced Plasticity (TRIP) steels. The microstructure of DP steels is composed of ferrite and martensite, while the microstructure of TRIP steels is a matrix of ferrite, in which martensite and/or bainite, and more than 5% retained austenite exist.

##### 4.1 Experiment

A square cylinder impacting experiment with the initial velocity of  $5m/s$ ,  $10m/s$ ,  $15m/s$  and  $20m/s$  is considered as shown in Fig.5. The values of geometry and related parameters shown in Fig.5 are listed in Tab.1. The evaluation is performed by commercial FEM analysis code LS-DYNA970. The FE model of the tube impact system as shown in Fig.6 consists of 2128 shell elements representing the cubic cylinder and 60 mass elements the sum of 600kg representing the concentrated mass attached to the end of the cylinder. Rigid wall is represented by stonewall feature of LS-DYNA. Numerical solutions in the progress of optimization are performed on IBM AIX5 computing platform. A single FE analysis of the cylindrical tube takes about 2.8 min with 8 processors.

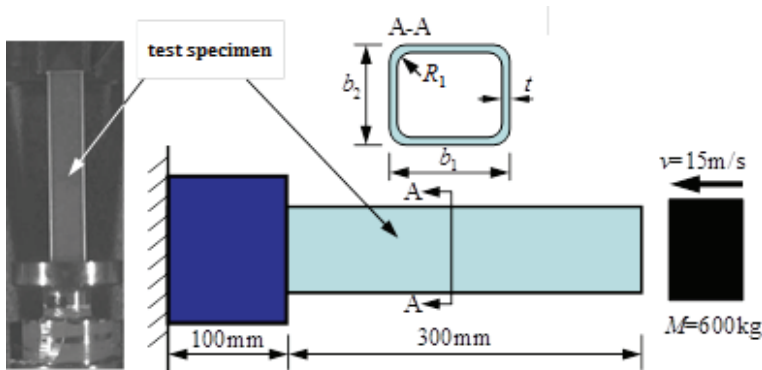


Figure 5: Experimental implementation of impacting initiators and corresponding sizes

Table 1: The parameters for impacting experiment

Parameter	$R_1$	$b_2$	$b_2$	$t$	$v$
Value	$3mm$	$60mm$	$60mm$	$1.2mm$	$15m/s$

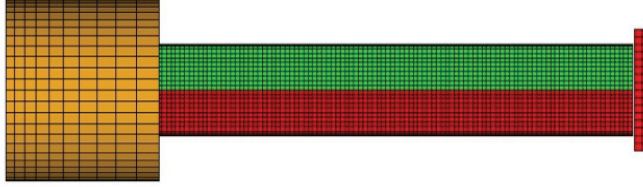


Figure 6: FE model of impacting experiment

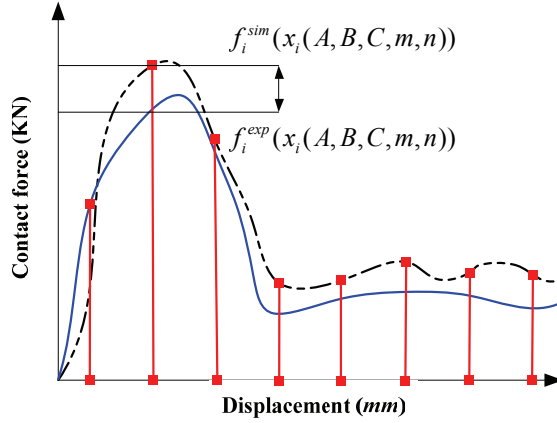


Figure 7: Definition Objective function

#### 4.2 Objective function

According to Eq.(1), there is a set of five model parameters that need to be identified:  $X = (A, B, C, m, n)$ . This is normally done through an inverse identification method by fitting the model to sets of experimental data. That is to minimize the Euclidean distance between the experimental data and those predicted by the material model via the FE solution as shown in **Fig.7**. As shown in **Fig.7**, the displacement can be divided into several uniformly pieces. Ten sample points are selected to estimate objective functions as

$$RSS_{Dyna}^j = \min \frac{1}{k} \left( \sum_{i=1}^k (f_i^{exp}(X) - f_i^{sim}(X))^2 \right) \quad (24)$$

where  $k$  denotes the total number of observations(sample points);  $RSS$  is the minimum value of one of the objective function which corresponds to the residual sum of squares of the fit. The subscript ‘Dyna’ refers to the rate and temperature depen-

dence of the response and  $j$  is the  $j$ th experiment. The multi-objective function can be expressed as

$$\min(RSS_{Dyna}^1, RSS_{Dyna}^2 \cdots RSS_{Dyna}^n). \tag{25}$$

Table 2: Performance criterions of inverse method for DP980

Performance criterions		Value
Initial sample points		15
Sum of number of samples		824
Number of samples evaluated by FE simulation		112
Number of samples predicted by the LS-SVR		712
Accurate criterions for the LS-SVR-based metamodel		
	$R^2$	0.932
	RAAE	0.082
	RMAE	0.356
	Variance of $R^2$	0.141
Pareto solution number		41
Convergence measure $\Upsilon$		0.0872
Diversity measure $\delta$		0.6834
Purity P		0.9213
$S_M$		0.1043

By consideration of reliability and according to Eq.(23), the Eq.(25) can be extended as

$$\min \sum_{j=1}^n \left\{ f_j \left( (RSS_{Dyna}^j)_\mu, (RSS_{Dyna}^j)_\sigma \right) \right\}. \tag{26}$$



### 4.3 DP980 parameter identification

According to Eq.(21), the updated multiobjective function for DP980 is formulated as

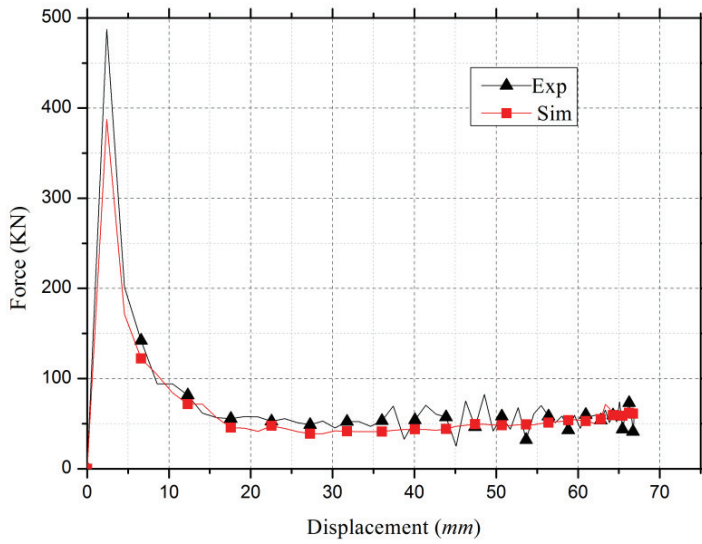
$$\left\{ \begin{array}{l} \min \sum_{j=1}^4 \left\{ f_j \left( (RSS_{Dyna}^j)_\mu, (RSS_{Dyna}^j)_\sigma \right) \right\} \\ s.t. \left\{ \begin{array}{l} 300\text{MPa} < A < 600\text{MPa} \\ 800\text{MPa} < B < 1600\text{MPa} \\ 0.003 < C < 0.050 \\ 0.30 < m < 3.00 \\ 0.10 < n < 0.85 \end{array} \right. \end{array} \right. \quad (27)$$

According to algorithm presented in Fig.1, the impacting experiment is carried out. Ten sample points are extracted from displacement-contact force curve as shown in Fig.7. Additionally, four experiments with different velocities,  $5m/s$ ,  $10m/s$ ,  $15m/s$  and  $20m/s$ , are implemented. Finally, 41 Pareto frontier sample points are generated. The performance related with metamodel are several statistic metrics R Square ( $R^2$ ), relative average absolute error (RAAE), relative mean absolute error (RMAE) and variance of  $R^2$  [Jin et al.(2001)]. The performance of the multiobjective algorithms is evaluated with respect to one or more of the four performance measures: the convergence measure  $\Upsilon$  [Bandyopadhyay et al. (2004)], diversity measure  $\delta$  [Deb et al. (2002)], purity  $P$  [Bandyopadhyay et al. (2004)] and minimal-spacing ( $S_M$ ) [Bandyopadhyay et al. (2004)]. For DP980 identification procedure, the performance criterions of inverse method are listed in Tab.2.

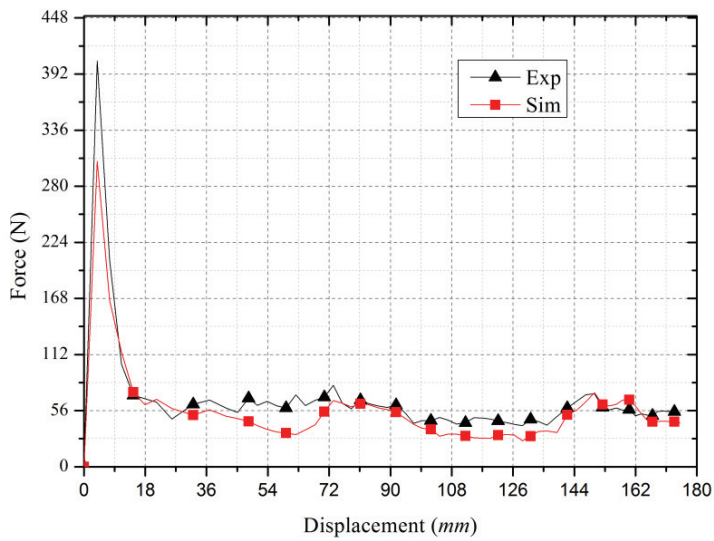
As we know, the final solution for material parameter identification is not unique. To extract the best solution from Pareto frontier, we substitute the Pareto solution into FE model and selected the best fit compared with simulation solution as shown in Tab.3. The comparisons between the FE simulations and experiments are demonstrated in Fig.8 and the crashed piece with  $15m/s$  is illustrated in Fig.9. Moreover, in order to verify the accuracy of the identified material parameters, simple experiments are also carried out, the strain-stress curve on strain-rate  $15s^{-1}$ ,  $200s^{-1}$ ,  $400s^{-1}$  are also obtained and compared with JC-model with identified by the proposed method as shown in Fig.10. It is obvious that the curves on different strain-rates are nearly matched.

### 4.4 TRIP780 parameter identification

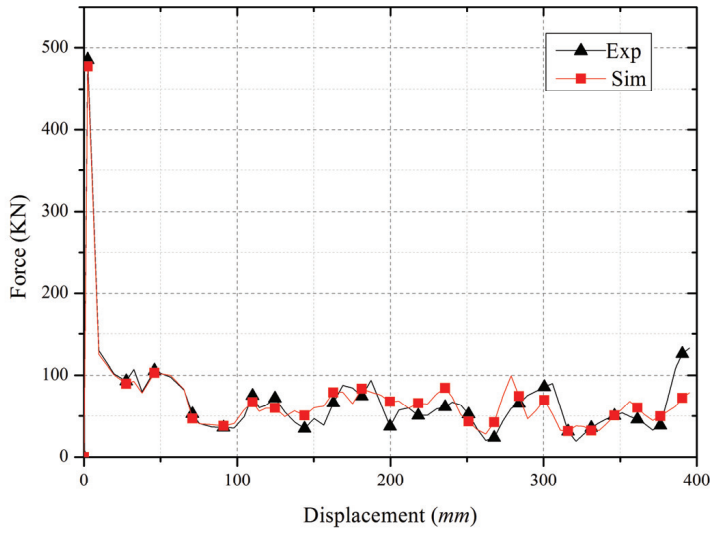
In order to verify the performance of the proposed inverse method, material parameters of TRIP590 are identified in this way. The obtained material parameters are



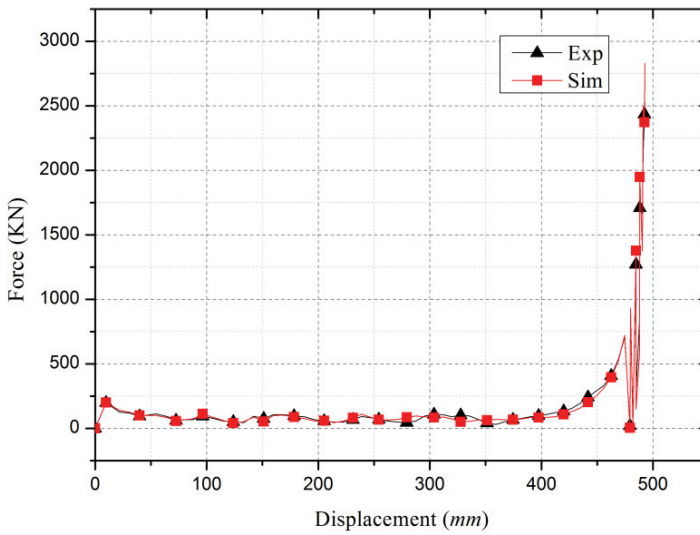
Velocity 5m/s



Velocity 10m/s



Velocity 15m/s



Velocity 20m/s

Figure 8: Comparisons between simulations and experiments based on 5m/s, 10m/s, 15m/s and 20m/s

Table 3: Performance criterions of inverse method for DP980

Performance criterions		Value
Initial sample points		15
Sum of number of samples		824
Number of samples evaluated by FE simulation		112
Number of samples predicted by the LS-SVR		712
Accurate criterions for the LS-SVR-based metamodel		
	$R^2$	0.932
	RAAE	0.082
	RMAE	0.356
	Variance of $R^2$	0.141
Pareto solution number		41
Convergence measure $\Upsilon$		0.0872
Diversity measure $\delta$		0.6834
Purity P		0.9213
$S_M$		0.1043



a). Simulation



b). Experiment

Figure 9: Comparison between simulation and experiment based on 15m/s

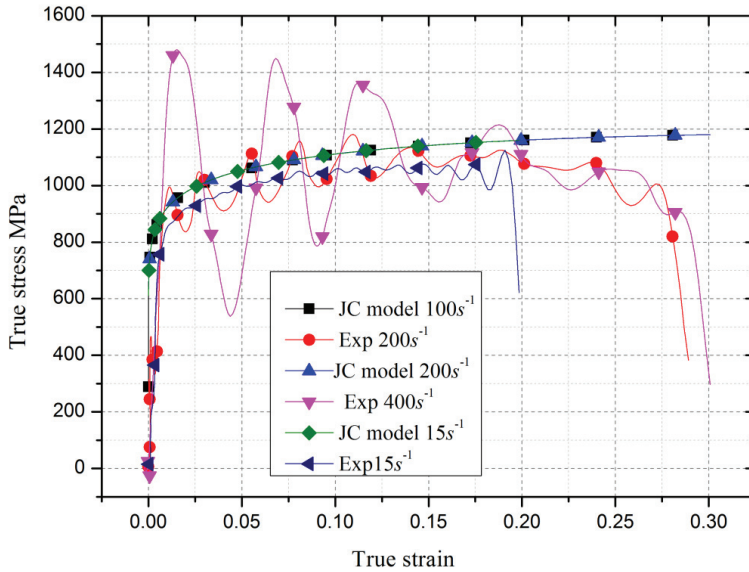


Figure 10: Comparisons between the JC-model and experiments for DP980

Table 4: The identified material parameters for DP980

JC parameters	<i>A</i>	<i>B</i>	<i>n</i>	<i>C</i>	<i>m</i>
Value	285.035	1127.94	0.128	0.0021	2.6215

presented in Tab.4. Four experiments with different velocities,  $5m/s$ ,  $10m/s$ ,  $15m/s$  and  $20m/s$ , are also implemented. We also compare the strain-stress curve between JC-model and simple experiments with  $15s^{-1}$ ,  $200s^{-1}$  and  $400s^{-1}$ . According to Fig.11, It is obvious that the curves on different strain-rates are nearly matched.

Table 5: The final identified material parameters for TRIP780

JC parameters	<i>A</i>	<i>B</i>	<i>n</i>	<i>C</i>	<i>m</i>
Value	438.67	1323.56	0.493	0.0122	2.6215

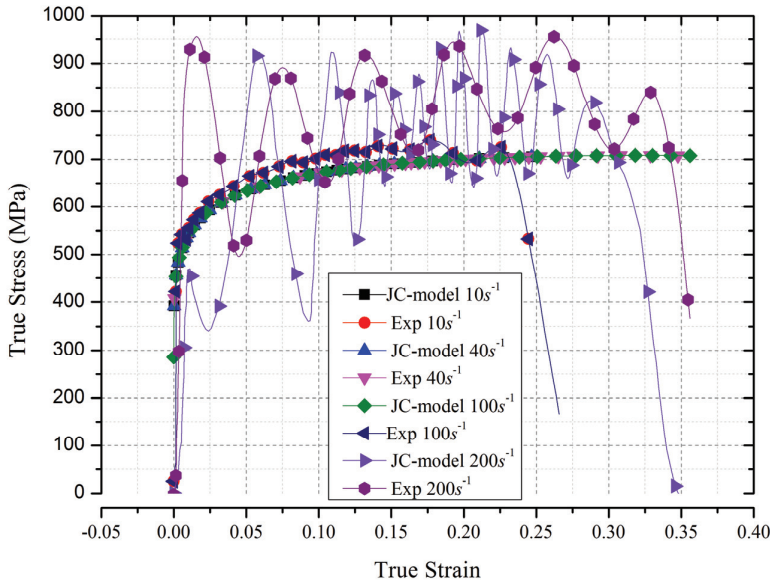


Figure 11: Comparisons between the JC-model and experiments for TRIP780

## 5 Conclusions

The purpose of this study is to propose a robust inverse method for material parameters of the AHSS. The characteristics of the suggested inverse technology can be summarized as follows.

1. Compared with the popular hybrid numerical methods, the mean values and standard deviations of the differences between the simulated and experimental data are used. Multi-samples are also used in identification. Therefore, the inverse method actually converted into a multi-objective optimization problem. Due to this feature, both robustness of the inverse method can be guaranteed;
2. In order to construct the global inverse method, the PSO is used for global searching. Considering the computational cost due to expensive evaluations, the metamodel technique is integrated with the PSO, that means the proposed inverse method actually is a metamodel-based inverse method;
3. Since the inverse method is based on metamodel technique, the robustness is

also determined by the characteristic of the model. Therefore, a robust model based on the SRM is proposed. The LS-SVR is used for construction of the robust model.

**Acknowledgement:** This work is supported by Project of National Science Foundation of China (NSFC) under the grant number 11172097,10902037; the National 973 Program of China under the grant number 2010CB328005; Program for New Century Excellent Talents in University (NCET-11-0131); Hunan Provincial Natural Science Foundation of China under the grant number 11JJA001; Fundamental Research Funds for the Central Universities, Hunan University.

## References

**Alexandrov N, Dennis J. E. J., Lewis R.M., Torczon V.** (1998): A trust region framework for managing the use of approximation models in optimization. *Struct. Optim.* 1, vol.15, no.1, pp: 16–23.

**Bandyopadhyay S., Pal S.K., Aruna B.**(2004): Multi-objective GAs quantitative indices and pattern classification. *IEEE Transaction on Systems Man and Cybernetics – Part B: Cybernetics*, vol. 34, pp. 2088–2099.

**Box G. P., Draper N. R.**(1969): *Evolutionary operation: A statistical method for process management*. Wiley, New York.

**Cardenas-Garcia, J. F., Ekwaro-Osire, S., Berg, J. M., Wilson, W. H.**(2005): Non-linear least-squares solution to the Moire' hole method problem in orthotropic materials Part II: Material elastic constants, *Experimental Mechanics*, vol. 45, no. 4, 314–324.

**Chen W, Allen J K, Schrage D. P., Mistree F.**(1997) Statistical experimentation methods for achieving affordable concurrent systems design. *AIAA J.* vol. 35, no. 5, pp.893–900.

**Cherkassky V, Ma Y.**(2004): Comparison of loss functions for linear regression. *Proceedings of the 2004 IEEE International Joint Conference on Neural Networks*, vol. 1, no.25-29, pp.400–405.

**Coello C., Pulido G., Lechuga M.**(2004): Handling multiple objectives with particle swarm optimization, *IEEE Transactions on Evolutionary Computation*, vol. 8, no. 3, pp. 256–279.

**Corne D.W., Jerram N.R., Knowles J.D., Oates M.J.**(2001): PESA-II: region-based selection in evolutionary multiobjective optimization. *Proceedings of the Genetic and Evolutionary Computing Conference (GECCO-2001)*, Morgan Kaufman, pp. 283–290.

**Deb K., Pratap A., Agarwal S., Meyarivan T.**(2002): A fast and elitist multi-objective genetic algorithm: NSGA-II, *IEEE Transactions On Evolutionary Computation*, vol. 6, no. 2, pp. 182–197.

**Deb K., Pratap A., Agarwal S., Meyarivan T.**(2002): A fast and elitist multi-objective genetic algorithm: NSGA-II. *IEEE Transactions On Evolutionary Computation*, vol. 6, no. 2, pp. 182–197.

**Dey S, Børvik T, Hopperstad O. S., Langseth M.**(2007): On the influence of constitutive relation in projectile impact of steel plates, *International Journal of Impact Engineering*, vol. 4, no. 3, pp. 464–86.

**Ghouati, O., Gelin, J.C.** (1997): An inverse approach for the identification of complex material behaviours. In: Sol, H., Oomens, C.W.J. (Eds.), *Material Identification using Mixed Numerical Experimental Methods*. Kluwer Academic Publishers, Dordrecht, pp. 93–102.

**Ghouati, O., Gelin, J.C.**(2001): A finite element-based identification method for complex metallic material behavior, *Computational Materials Science*, vol. 21, no. 1, pp. 57–68.

**Goldberg D.**(1989): *Genetic algorithms in search, optimisation, and machine learning*. New York: Addison-Wesley.

**Grediac, M.**(2005): The use of full-field measurement methods in composite material characterization: interest and limitations, *Composites: Part A* vol. 35, pp.751–761.

**Holland J.H.**(1975): *Adaptation in natural and artificial systems*. Ann Arbor (MI): University of Michigan Press.

**Huang, L., Sun, X., Liu, Y., Cen, Z.**(2004): Parameter identification for two-dimensional orthotropic material bodies by the boundary element method, *Engineering Analysis with Boundary Elements*, vol. 28, pp. 209–221.

**Jin R., Chen W, Simpson T.W.**(2001): Comparative studies of metamodeling techniques under multiple modeling criteria. *Structural and Multidisciplinary Optimization*, vol. 23, no. 1, pp. 1-13.

**Johnson G.R., Cook W.H.**(1983): A constitutive model and data for metal subjected to large strains, high strain rates and high temperatures. In: *Proceedings of the Seventh Symposium on Ballistics*, Hague, Netherlands, pp.541–47.

**Kajberg, J., Lindkvist, G.**(2004): Characterization of materials subjected to large strains by inverse modelling based on in-plane displacement fields, *International Journal of Solids and Structures*, vol. 41, no. 13, pp. 3439–3459.

**Kennedy J., Eberhart R.**(1995): Particle swarm optimization, *Proceedings of the IEEE International Conference on Neural Networks*, vol. 4, pp.1942–1948.



- Langrand B, Geoffroy P, Petitniot J-L, Fabis J, Markiewicz E, Drazetic P.** (1999): Identification technique of constitutive model parameters for crashworthiness modelling. *Aerospace Science and Technology*, vol. 4, no. 3, pp. 215–27.
- Langrand B., Geoffroy P., Petitniot J. L., Fabis J., Markiewicz E., Drazetic P.**(1999): Identification technique of constitutive model parameters for crashworthiness modelling. *Aerospace Science and Technology*, vol 4, pp. 215–27.
- Mangono P. L.** (1999): *The principles of materials selection for engineering design*. New Jersey: Prentice Hall.
- Molomard, J., Le Riche, R., Vautrin, A., Lee, J.R.**(2005): Identification of the four orthotropic plate stiffnesses using a single open-hole tensile test, *Experimental Mechanics*, vol. 45, no. 5, pp. 404–411.
- Raquel C, Naval P.**(2005): An effective use of crowding distance in multiobjective particle swarm optimization, *Proceedings of the 2005 conference on genetic and evolutionary computation*, Washington (DC, USA).
- Shi Y., Eberhart R.**(1998): Parameter selection in particle swarm optimization, *Proceedings of Evolutionary Programming*, pp. 591–600.
- Suykens J. A. K., Vandewalle J.**(1999): Least Squares Support Vector Machine Classifiers. *Neural Processing Letters*, 1999; vol. 9, no. 3, pp. 293-300.
- Toropov V, van Keulen F, Markine V, de Doer H.** (1996): Refinements in the multi-Point approximation method to reduce the effects of noisy structural responses. *Proceedings 6th AIAA/USAF/NASA/ISSMO Symposium on Multidisciplinary Analysis and Optimization*, Vol. 2, Bellevue, WA.
- Wang G.G, Dong Z., Aitchison P.**(2001): Adaptive response surface method-a global optimization scheme for computation-Intensive design problems. *Eng. Optim.* ,vol. 33, no. 6, pp.707–734.
- Wang, W.T., Kam, T.Y.**(2004): Material characterization of laminated composite plates via static testing, *Composite Structures*, vol 50, pp. 347–352.
- Wang, Z., Cardenas-Garcia, J. F., Han, B.**(2005): Inverse method to determine elastic constants using a circular disk and Moire' interferometry. *Experimental Mechanics*, vol. 45, no. 1, 27–34.
- Wang H., Li E., Li G. Y.**(2010): Probability-based least square support vector regression metamodeling technique for crashworthiness optimization problems. *Computational Mechanics*, vol. 47, no. 3, pp. 251-263.
- Wang, H, Li GY, Zhong Z. H.**(2008a): Optimization of sheet metal forming processes by adaptive response surface based on intelligent sampling method, *J. Mater. Process. Tech.* vol, 197, no, 1-3, pp. 77-88.
- Wang H, Li E, Li GY, Zhong ZH.**(2008b): Development of metamodeling based

optimization system for high nonlinear engineering problems. *Adv Eng Softw*, vol. 39, no. 8., pp.629-645.

**Wu C. H., Ho M.J., Lee D.T.**(2003): Travel time prediction with support vector regression. *IEEE Transactions on Intelligent Transportation Systems* vol. 5. pp. 276–81.

**Wujek B.A, Renaud J.E.**(1998a): New adaptive move-limit management strategy for approximate optimization Part 1. *AIAA J.*, vol. 36, no. 10, pp.1911–1921.

**Wujek B.A, Renaud J.E.**(1998b): New adaptive move-limit management strategy for approximate optimization Part 2, *AIAA J*, vol. 36, no. 10, 1922–1934.

**Yang H, Chan L, King I.**(2002a): Support vector machine regression for volatile stock market prediction. *IDEAL 2002, Lecture notes in Computer Science*, vol. 2412. Berlin: Springer, pp. 391–6.

**Yang H, King I, Chan L.**(2002b): Non-fixed and asymmetrical margin approach to stock market prediction using support vector regression. *Proceedings of the international conference on neural information processing (ICONIP2002)*, Singapore.

**Zitzler E., Laumanns M., Thiele L.**(2001): SPEA2: Improving the strength Pareto evolutionary algorithm. *Technical report TIK-103, Computer Engineering and Network Laboratory (TIK)*, Swiss Federal Institute of Technology (ETH), Gloriastrasse 35, CH-8092 Zurich, Switzerland, May 2001.